



**CHALMERS**  
UNIVERSITY OF TECHNOLOGY

## **Analyses of long-term fungal degradation of spruce bark reveals varying potential for catabolism of polysaccharides and extractive compounds**

Downloaded from: <https://research.chalmers.se>, 2026-04-05 10:04 UTC

Citation for the original published paper (version of record):

Sörensen Ristinmaa, A., Korotkova, E., Arntzen, M. et al (2024). Analyses of long-term fungal degradation of spruce bark reveals varying potential for catabolism of polysaccharides and extractive compounds. *Bioresource technology*, 402. <http://dx.doi.org/10.1016/j.biortech.2024.130768>

N.B. When citing this work, cite the original published paper.



# Analyses of long-term fungal degradation of spruce bark reveals varying potential for catabolism of polysaccharides and extractive compounds

Amanda S. Ristinmaa<sup>a</sup>, Ekaterina Korotkova<sup>b</sup>, Magnus Ø. Arntzen<sup>c</sup>, Vincent G. H. Eijsink<sup>c</sup>, Chunlin Xu<sup>b</sup>, Anna Sundberg<sup>b</sup>, Merima Hasani<sup>d,e</sup>, Johan Larsbrink<sup>a,e,\*</sup>

<sup>a</sup> Chalmers University of Technology, Department of Life Sciences, Division of Industrial Biotechnology, SE-412 96 Gothenburg, Sweden

<sup>b</sup> Abo Akademi University, Laboratory of Natural Materials Technology, FI-20500 Abo, Finland

<sup>c</sup> Faculty of Chemistry, Biotechnology and Food Science, Norwegian University of Life Sciences (NMBU), NO-1433 Ås, Norway

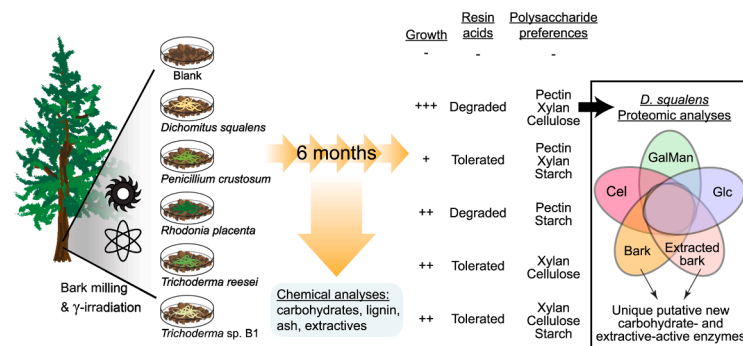
<sup>d</sup> Department Chemistry and Chemical Engineering, Chalmers University of Technology, SE-412 96 Gothenburg, Sweden

<sup>e</sup> Wallenberg Wood Science Center, Chalmers University of Technology, SE-412 96 Gothenburg, Sweden

## HIGHLIGHTS

- Growth of wood-rot and mold fungi on spruce bark was assessed over six months.
- Degradation of carbohydrates, lignin, and extractives was monitored and quantified.
- The fungi use varying degradation strategies when growing on spruce bark.
- *Dichomitus squalens* produces many proteins of unknown function when growing on bark.

## GRAPHICAL ABSTRACT



## ARTICLE INFO

**Keywords:**  
White-rot fungi  
Resin acids  
Proteomics  
CAZyme

## ABSTRACT

The bark represents the outer protective layer of trees. It contains high concentrations of antimicrobial extractives, in addition to regular wood polymers. It represents a huge underutilized side stream in forestry, but biotechnological valorization is hampered by a lack of knowledge on microbial bark degradation. Many fungi are efficient lignocellulose degraders, and here, spruce bark degradation by five species, *Dichomitus squalens*, *Rhodonia placenta*, *Penicillium crustosum*, *Trichoderma sp. B1*, and *Trichoderma reesei*, was mapped, by continuously analyzing chemical changes in the bark over six months. The study reveals how fungi from different phyla degrade bark using diverse strategies, regarding both wood polymers and extractives, where toxic resin acids were degraded by Basidiomycetes but unmodified/tolerated by Ascomycetes. Proteome analyses of the white-rot *D. squalens* revealed several proteins, with both known and unknown functions, that were specifically upregulated during growth on bark. This knowledge can accelerate improved utilization of an abundant renewable resource.

\* Corresponding author.

E-mail address: [johan.larsbrink@chalmers.se](mailto:johan.larsbrink@chalmers.se) (J. Larsbrink).

<https://doi.org/10.1016/j.biortech.2024.130768>

Received 17 November 2023; Received in revised form 26 April 2024; Accepted 29 April 2024

Available online 30 April 2024

0960-8524/© 2024 The Author(s). Published by Elsevier Ltd. This is an open access article under the CC BY license (<http://creativecommons.org/licenses/by/4.0/>).

## 1. Introduction

Bark is the outmost tissue of the tree, protecting it against abiotic stress, animal attack, and microbial degradation. It accounts for around 10–15 % of the volume at harvest, and ca 400 million m<sup>3</sup> of bark are produced annually in the Nordic countries (Kwan et al., 2022), which mills and factories burn for energy. Similar to wood, the bark consists of lignin, hemicelluloses, and cellulose, but it is also enriched in so-called extractive compounds (extractives), which can be strongly antimicrobial. Extractives can vary greatly in types and amounts among tree species, growth stages, and seasons (Ek et al., 2009). A softwood tree of high industrial value in the northern hemisphere is spruce. Its bark has a low dry matter content compared to wood (Kempainen et al., 2014), making direct combustion inefficient, but it is enriched in diverse and potentially valorizable extractives including triglycerides, steryl esters, sterols, resin acids, and fatty acids (Krogell et al., 2012), the most abundant of which are resin acids (~12 mg/g bark) that can be highly toxic due to interactions with biological membranes (Ek et al., 2009). The second-most abundant extractives are sterols, with  $\beta$ -sitosterol as the main compound.

Polysaccharides constitute ~40 % (w/w) of spruce bark, but in addition to the expected wood polysaccharides, cellulose and hemicelluloses, the bark also contains notable amounts of starch and pectin (Krogell et al., 2012; Le Normand et al., 2012; Le Normand et al., 2021). Of the bark dry weight, cellulose accounts for ~20–30 %, and starch accounts for 0.5 to several percent (Fengel & Wegener, 1984; Krogell et al., 2012). The primary hemicellulose in softwood is galactoglucomannan (GGM), and it accounts for ~10 % of the bark dry weight (Fengel & Wegener, 1984). The second most abundant hemicellulose in bark is glucuronarabinoxylan (GAX), accounting for ~6 % of the bark dry weight (Fengel & Wegener, 1984). Pectins – homogalacturonan, xylogalacturonan, and rhamnogalacturonans (RG-I and RG-II) – comprise 3–7 % of the bark dry weight (Fengel & Wegener, 1984; Yadav et al., 2023).

Basidiomycetes and Ascomycetes are recognized as major lignocellulose degraders. Within Basidiomycota, lignocellulolytic species can be classified as brown- or white-rot types depending on their effect on the wood. Brown-rot fungi rapidly depolymerize wood carbohydrates without significant removal of the brown lignin, in contrast to white-rot fungi, that simultaneously degrade all wood components, including lignin (Daly et al., 2018). Ascomycota includes well-known cellulase producers such as *Trichoderma*, *Aspergillus*, and *Penicillium*, and these can exhibit so-called soft-rot, whose rot leads to an overall softened wood structure.

Extensive studies on lignocellulose degradation have enabled advanced utilization technologies based largely on fungal degradative enzymes. For bark, similar broad studies are lacking and the high amounts of extractive compounds in the bark make direct comparisons questionable. A recent study showcased how mixed microbial communities can degrade bark over several months, pointing out resin acids as key molecules limiting community diversification and showing that their degradation is linked to bacterial activity (Ristinmaa et al., 2023). The roles fungi play in bark degradation remain unclear. The white-rot fungi *Phanerochaete velutina* and *Stropharia rugosoannulata* have been found to degrade hemicelluloses, cellulose, and certain extractives when grown on Scots pine bark, though the analyses were limited to initial degradation stages (Valentín et al., 2010). The brown-rot fungus *Rhodonía placenta* (formerly *Postia placenta*) has been shown to degrade resin acids (Belt et al., 2017), and the white-rot fungus *Phlebiopsis gigantea* has been shown to metabolize non-toxic bark triglycerides (Hori et al., 2014). There are no studies comparing the growth of multiple filamentous fungi, from both Asco- and Basidiomycota, on spruce bark over long timespans, with simultaneous monitoring of the resulting chemical changes to the bark.

In the present study, the aim was to deepen the understanding of how spruce bark can be degraded by fungi, using long incubation times (six

full months) to mimic natural conditions. Five species were selected based on the ability to grow on the bark, and a hypothesis that different rot types would use distinct strategies: *Dichomitus squalens* (white-rot), *R. placenta* (brown-rot), *Trichoderma reesei* (soft-rot), *Penicillium crustosum* (mold), and a new *Trichoderma* strain isolated from a spruce tree stump. Given the lack of previous data on fungal spruce bark degradation, the bark deconstruction was followed broadly, where fungal growth was assessed through mass-loss analyses, and then coupled to broad chemical compositional analyses to evaluate effects on bark extractives, lignin, and polysaccharides over time. *D. squalens* was found to be the most efficient overall bark degrader and it was studied in more detail, revealing a remarkable proficiency in degrading hemicelluloses and pectin, the primary non-cellulosic polysaccharides found in spruce bark. Further proteomic analysis of its secretome during bark deconstruction revealed putative novel extractive-degrading enzymes and carbohydrate-active enzymes (CAZymes) likely involved in bark degradation.

## 2. Material and methods

### 2.1. Maintenance and identification of fungi

Dikaryotic *Dichomitus squalens* FBCC312 (CBS 432.34), *Rhodonía placenta* (CBS 447.48), *Trichoderma reesei* (NCIM 1186), *Penicillium crustosum* (FRR 1669) were maintained on Potato dextrose agar (PDA) plates (Sigma). The fungal strain B1 was isolated from a spruce tree stump just below partly degraded bark (summer 2019, Hälsingland county, Sweden), cultivated on PDA plates, and identified by extracting genomic DNA using the NucleoSpin Soil kit (Macherey-Nagel), PCR amplifying the internally transcribed spacer (ITS) gene region using primers ITS1 (5'-TC CGT AGG TGA ACC TGC GG-3') and ITS4 (5'-TCC TCC GCT TAT TGA TAT GC-3'), and the EF1- $\alpha$  gene using primers EF1-728F (5'-CAT CGA GAA GTT CGA GAA GG-3') and EF1-986R (5'-TAC TTG AAG GAA CCC TTA CC-3') in 50  $\mu$ L PCR mixtures with Maxima Hot Start PCR Master Mix (Thermo), 0.5  $\mu$ M of each primer, and 1  $\mu$ L of extracted genomic DNA, following: 94 °C for 3 min, 30 cycles of 94 °C for 30 s, 55 °C for 30 s, and 72 °C for 1 min, and a final extension at 72 °C for 10 min. Sequenced PCR products (Macrogen) were BLAST compared to GenBank entries. The closest matches were *Trichoderma atroviride* (98.89 % seq. id., 99 % query cover for EF1- $\alpha$ ) and *T. paraviridescens* (100 % seq. id. and cover for ITS).

### 2.2. Fungal cultivation on spruce bark

From an approximately 50-year old tree, fresh spruce bark was collected, partially dried, milled in a Wiley-type mill, mesh size < 0.1 mm, and sterilized by gamma-irradiation (25 kGy, Mediscan GmbH & Co KG) to avoid autoclave-induced chemical changes. For each fungus, static liquid pre-cultures in 250 mL Erlenmeyer flasks containing 50 mL potato dextrose broth (Sigma) were inoculated from PDA plates with three agar plugs (0.5 cm diameter) and incubated for 7 days at 20 °C. Mycelium from two pre-cultures was fished out and transferred to a blender cup filled with 150 mL basal medium (4 g/L KH<sub>2</sub>PO<sub>4</sub>, 13.6 g/L (NH<sub>4</sub>)<sub>2</sub>SO<sub>4</sub>, 0.8 g/L CaCl<sub>2</sub>·2H<sub>2</sub>O, 0.6 g/L MgSO<sub>4</sub>·7H<sub>2</sub>O, 10 mg/L FeSO<sub>4</sub>·7H<sub>2</sub>O, 3.2 mg/L MnSO<sub>4</sub>·H<sub>2</sub>O, 2.8 mg/L ZnSO<sub>4</sub>·7H<sub>2</sub>O, 4 mg/L CoCl<sub>2</sub>·6H<sub>2</sub>O) and blended in a Waring blender for 10 s at 8000 rpm three times with a 30 s pause in between each blending (Daly et al., 2018). 1 mL blended preculture was mixed with 35 mL of basal medium in a 50-mL tube and added to 10 g of sterilized bark on plates, which were then weighed. Abiotic controls were prepared similarly. To mitigate effects of evaporation during the cultivation, samples were weighed and supplemented with Milli-Q water when necessary. Five cultures were incubated statically at 20 °C for each time-point (8 over 24 weeks): three for compositional analysis experiments and two for mass loss measurements. Fungal-caused mass loss was assessed by drying samples for three days at 60 °C, weighing, and comparison of the weights of biotic samples

to the starting material and abiotic controls.

### 2.3. Compositional analysis of spruce bark

Compositional analyses were assessed based on the percent change compared to the control (blank) sample measured at the same week using Equation (1), below.

$$\%Change = \frac{X_1 - X_{mean}^b}{X_{mean}^b} \quad (1)$$

$X_1$  = measured values at week  $y$ ;  $X_{mean}^b$  = mean of the three blank samples at week  $y$

#### 2.3.1. Extractive extraction, analysis, and quantification

Soxhlet extraction with acetone was used to obtain spruce bark extractives, as previously described (Ristinmaa et al., 2023). Gas chromatography coupled to mass spectrometry (GC-MS; Agilent 7890A and Agilent 5975C) with a quadrupole was used to identify and quantify individual bark extractives, using an internal methyl heptadecanoic standard and pure external standards. Fatty acids were quantified against hexadecenoic acid, resin acids against dehydroabietic acid, and  $\beta$ -sitosterol against pure standard. Response factors for isopimarane type resin acids were determined by silylation and GC analysis on two samples with equal amounts of 0.1 mg/L isopimaric acid, hexadecenoic acid, and dehydroabietic acid. Extractive samples were dissolved in acetone to 10 mg/mL. From this, 300  $\mu$ L was mixed with 200  $\mu$ L of internal standard (methyl heptadecanoic acid, 1 mg/mL) in acetone. The extracts and standards were then derivatized with 100  $\mu$ L *N*-Methyl-*N*-(trimethylsilyl)trifluoroacetamide, heated 20 min at 70 °C, and analyzed as trimethylsilyl derivatives. Helium was used as carrier gas with a flow rate of 1 mL/min. The MS source was operated at 230 °C and the quadrupole at 150 °C. Analytes were separated using a HP-5 column (Agilent) with an injector temperature set to 300 °C, the temperature program starting at 70 °C, held for 2.25 min, then increased to 200 °C at 20 °C/min, and then increased to 230 °C at 5 °C/min. A final ramp of 35 °C/min to 300 °C was held for 10 min. The NIST MS Search Program (v. 2.2) was used for identification using the NIST/EPA/NIH Mass Spectral Library (NIST 11), in addition to external standards (see supplementary material).

#### 2.3.2. Ash and protein content

The proportion of ash was measured according to the National Renewable Energy Laboratory standard method as previously described (Ristinmaa et al., 2023). The protein content of the acetone extracted bark was derived from nitrogen content determination using carbon, hydrogen, nitrogen, and sulfur combustion analysis (Elementar vario MICRO cube), with helium as the carrier gas, using ~2 mg dry bark (105 °C overnight incubation) samples. Calibration was done using sulphanylamine (Elemental Microanalysis), and combustion and reduction were conducted at 1,150 and 850 °C, respectively. The protein content was estimated by multiplying the measured nitrogen content with the nitrogen to protein conversion factor 6.25 (Jones, 1931).

#### 2.3.3. Chemical characterization of carbohydrates and lignin

Dry acetone-extracted bark (105 °C overnight incubation) was hydrolyzed in 72 % (w/w) sulfuric acid, and monosaccharide concentrations determined using an internal fucose standard and pure external monosaccharide standards, by high-performance anion exchange chromatography with pulsed amperometric detection (HPAEC-PAD). Peak analysis was done in Chromeleon 7.2.10 (Thermo Scientific). Starch was analyzed using the total starch assay kit from Megazyme (Ireland), after drying samples for three days at 50 °C to prevent formation of retrograde starches and using four-fold lower sample amounts than in the standard protocol. Glucose concentrations were determined by HPAEC-PAD, as described above. For methanolysis, 10 mg freeze-dried bark samples

were used and analyzed as silylated sugars by GC, with resorcinol used as an internal standard (Krogell et al., 2013).

### 2.4. Proteomic sample preparation and analysis

The monokaryotic *D. squalens* strain CBS 464.89 (direct offspring of dikaryon FBCC312; Westerdijk Fungal Biodiversity Institute), was maintained on plates with 2 % (w/v) malt extract and 1.5 % (w/v) malt extract agar (Sigma). Two-layer agar plates including a filter disc were prepared as previously described (Bengtsson et al., 2016), using sterile QM-A Quartz filters, 47 mm diameter (Cytiva) to facilitate separation of cells and secreted proteins, including basal medium (see above), 1.5 % (w/v) agar, and 10 g/L carbon source: spruce bark, acetone-extracted spruce bark (extractive free), glucose (Sigma), galactomannan (Sigma), or cellulose (Sigma, microcrystalline, powder, 20  $\mu$ m), respectively. Secretomes from cells grown on plates were collected after 9 days (Lorentzen et al., 2021), by punching out a disc of agarose (~2 mL) between the underside of the agarose and the filter using a 50-mL tube. 100  $\mu$ L of 10 % sodium dodecyl sulfate/20 mM dithiothreitol/100 mM Tris-HCl pH 7.9 was added to each disc, the agarose melted by incubating at 95 °C for 10 min, vortexed vigorously, and after cooling to room temperature centrifuged 10 min at 5000 g through an Ultrafree DA assembly filter (Merck Millipore). The liquid fraction was transferred to another tube and the volume reduced to 25  $\mu$ L using a vacuum concentrator, and an equal amount (25  $\mu$ L) of Nu-Page buffer was added. The proteins were subjected to sodium dodecyl sulfate polyacrylamide gel electrophoresis at 270 mV for 5 min, using a Mini-Protean TGX Stain-free Protein gel (Bio-Rad Laboratories), and TGS as running buffer (Invitrogen), proteins stained with Coomassie blue (Thermo Fisher Scientific) and bands cut out and transferred to Eppendorf tubes (Sigma-Aldrich) and washed with Milli-Q water. Trypsin digestion was done as previously described (Bengtsson et al., 2016). Tryptic peptides were analyzed by liquid chromatography combined with mass spectrometry (LC-MS/MS; 5  $\mu$ L per injection) as described previously (Lorentzen et al., 2021), using a Dionex Ultimate 3000 nanoLC-MS/MS system connected to a Q-Exactive mass spectrometer (Thermo Scientific) with a nano-electrospray ion source.

MS raw files were analyzed using MaxQuant (v2.4.2.0) and proteins identified and quantified using the MaxLFQ algorithm. The data were searched against the UniProt proteome of *D. squalens* (UP000292082; 15,221 sequences) supplemented with common MS and proteomics contaminants such as keratins and bovine serum albumin. Reversed sequences of all protein entries were concatenated to the database for estimation of false discovery rates (FDR). The tolerance levels for matches were 6 ppm for MS and 20 ppm for MS/MS. Two missed trypsin cleavages were allowed. Protein N-terminal acetylation, oxidation of methionines, deamidation of asparagines and glutamines and formation of pyro-glutamic acid at N-terminal glutamines were allowed as variable modifications. The 'match between runs' feature of MaxQuant was applied with default settings. Only proteins present in  $\geq 2$  of the three biological replicates per growth substrate, after filtering all search results to reach a protein FDR of 1 %, were used for further analysis. Perseus v.1.6.1.1 was used for data analysis and R v.2023.03.0 was used for visualization. Protein secretion was predicted by combining three prediction algorithms: SignalP v.6.0 and Phobius (default parameters for eukaryotes), and WolfSort using a fungal prediction pattern (Horton et al., 2007; Käll et al., 2004; Teufel et al., 2022). Proteins were considered secreted if predicted by at least two algorithms. Protein names were assigned by UniProt and further annotated with CAZy family numbers using dbCAN2 (Zhang et al., 2018) with CAZy hidden Markov models, Enzyme Commission numbers and Gene Ontology terms, downloaded from UniProt.

### 3. Results and discussion

#### 3.1. Fungal growth on spruce bark

All five Basidiomycota and Ascomycota fungi grew visibly over the 24-week growth experiment (Fig. 1). A new fungal strain was used in the study, sourced from a spruce tree stump (underneath the bark). Sequencing showed it being a *Trichoderma* species, which was designated as *Trichoderma* sp. B1; its ITS and EF1- $\alpha$  sequences have been deposited in NCBI under accession numbers OQ875786 and OQ918064,

respectively. The growth of microorganisms was assessed over time by measuring the overall mass loss of the samples by comparison to the initial weights. Regardless of the fungus used, clear degradation of the bark was observed, though the extent of mass loss varied among the fungi. *D. squalens* caused the highest mass loss, with 30 % at the end of the experiment and reaching an apparent stationary phase (i.e., minor additional weight loss) within 12 weeks. For *T. reesei*, the total mass loss reached 20 % and stationary phase was reached within 16 weeks, while *Trichoderma* sp. B1 reached 26 % mass loss but only reached a stationary phase after 20 weeks. Compared to the other fungi, *R. placenta*

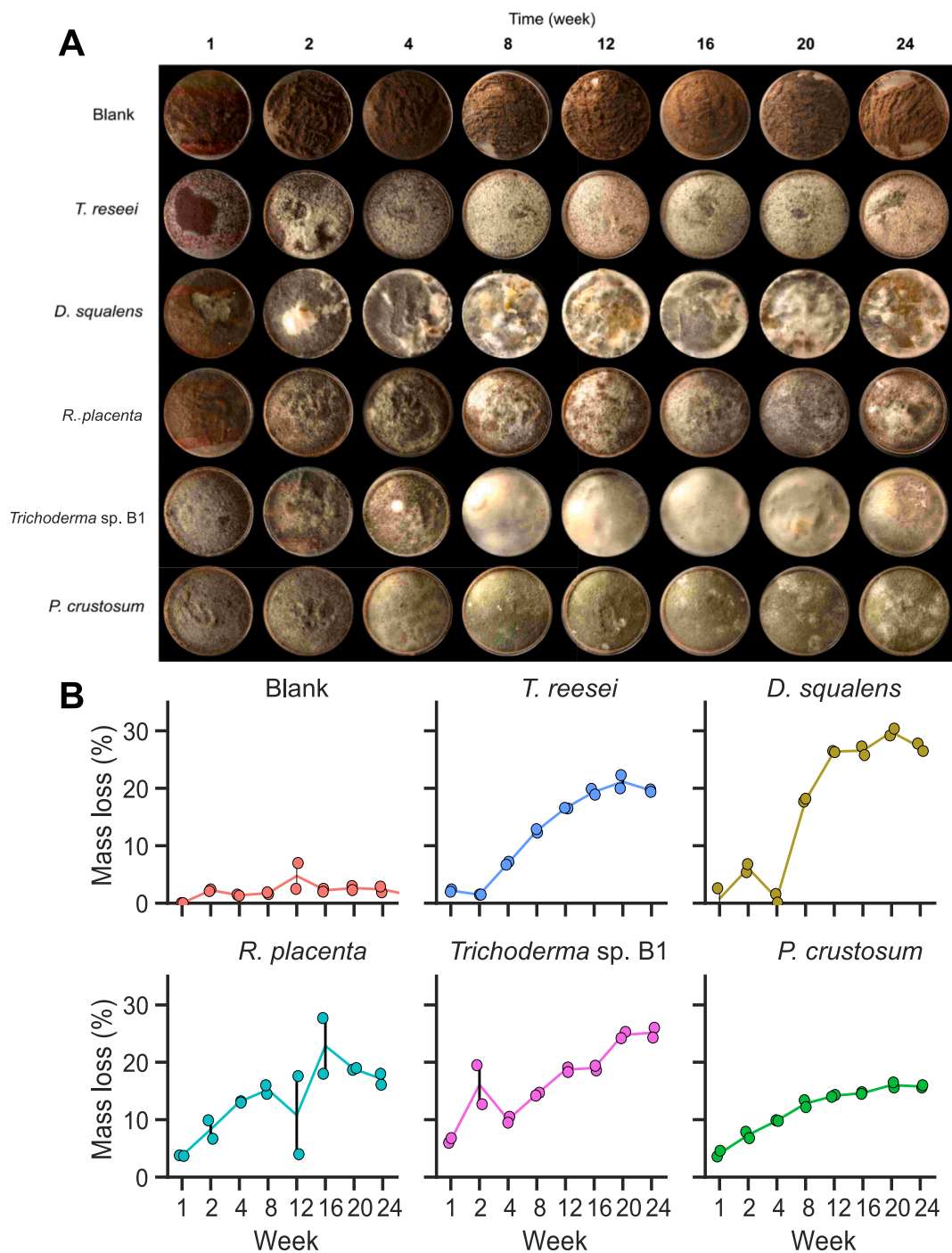


**Fig. 1.** Growth of filamentous fungi on spruce bark over six months (24 weeks), with the bark as the sole carbon source. No fungus was added to the blank sample. The plates were incubated at 20 °C. A) Representative plates from growth on bark. B) Mass loss for the different fungi. Individual data point measurements from biological duplicate experiments are shown and the line displays the mean.

and *P. crustosum* showed shorter lag phases, which indicates quick colonization of the bark. The total mass loss for *R. placenta* was comparable to *T. reesei* (~20 %), but the fast bark colonization of *P. crustosum* surprisingly caused the lowest overall mass loss (14 %) of the fungi. It is important to note that the actual degradation of the bark is higher than the observed mass loss. Part of the bark is lost to volatile compounds such as CO<sub>2</sub> (observed mass loss), and part is converted to fungal biomass that cannot easily be separated from the bark.

The distinct growth profiles of the fungi (Fig. 1) suggest different substrate preferences, which was further evaluated through compositional analyses of the bark. The observed variations in growth may also reflect differences in tolerance to extractives, as many are known to inhibit growth (Belt et al., 2017). The influence of the bark's general quality (e.g. moisture, mineral content) on degradability by these and other fungal species would be relevant to pursue in future studies. Protein content can be used to estimate fungal growth and indeed increased in all samples (Fig. 2), with the highest final protein content observed for *D. squalens*, again suggesting better growth than to the other fungi.

### 3.2. Bark decomposition

Compositional analysis was done for three time points (week 0, 12, and 24), representing early-, mid-, and late stages of degradation. In correlation with the observed mass loss in the samples, the proportional ash content increased significantly in all biotic samples compared with the uninoculated control, indicating significant loss of material in the form of CO<sub>2</sub> or other volatiles (Fig. 2; see supplementary material). *D. squalens*, *T. reesei*, and *Trichoderma* sp. B1 exhibited the highest relative ash content increase: up to 40 % at week 24 (Fig. 2). All measured compounds were evaluated against the total amount of ash rather than the dry bark weight, to account for the mass lost as volatiles, as in previous long-term bark degradation studies by microbial consortia (Ristinmaa et al., 2023). Lignin degradation was evaluated by measuring Klason and acid-soluble lignin (Fig. 2). Over time, the content of acid-soluble lignin decreased in samples treated with *D. squalens* and *Trichoderma* sp. B1, while it increased in samples treated with the other fungi. In contrast, Klason lignin degradation was minimal, even for well-known degraders of lignin such as *D. squalens* (Daly et al., 2018). Only minor evidence of degradation of Klason lignin was observed for the two Ascomycetes *P. crustosum* (after 12 weeks) and *T. reesei* (after 24 weeks). The exact content of the lignin fractions would require detailed analyses, e.g. 2D-NMR, to discern what the apparent changes in acid-soluble lignin stem from.

### 3.3. Degradation of extractives

The bark extractives, which are known for their antimicrobial properties, were expected to undergo modification and/or degradation during fungal growth. Indeed, a significant decrease in the total extractive content was seen across all fungal cultures (Fig. 2). To gain further insight into changes in specific extractives, additional analysis was conducted using GC-MS to monitor the most abundant fatty acids, resin acids, and sterols, which were identified using standards if available (hexadecanoic acid, isopimaric acid, dehydroabietic acid, abietic acid,  $\beta$ -sitosterol) or putatively identified by using the NIST library (9,12-octadecadienoic acid, octadecanoic acid, pimaric acid, 7-oxodehydroabietic acid, and ergosterol). All compounds identified by NIST had a match factor above 800, except ergosterol (716). For the ten components assessed, all fungi caused either an increase or a decrease of at least one of the compounds, compared to the abietic control. Changes in the contents of four selected compound types, with representatives from abietane and pimarane type resin acids, fatty acids, and sterols, are shown in Fig. 2. All the identified fatty acids (hexadecanoic acid, 9,12-octadecanoic acid, *trans*-9-octadecenoic acid) appeared to be readily available carbon sources for all fungi and were nearly entirely consumed

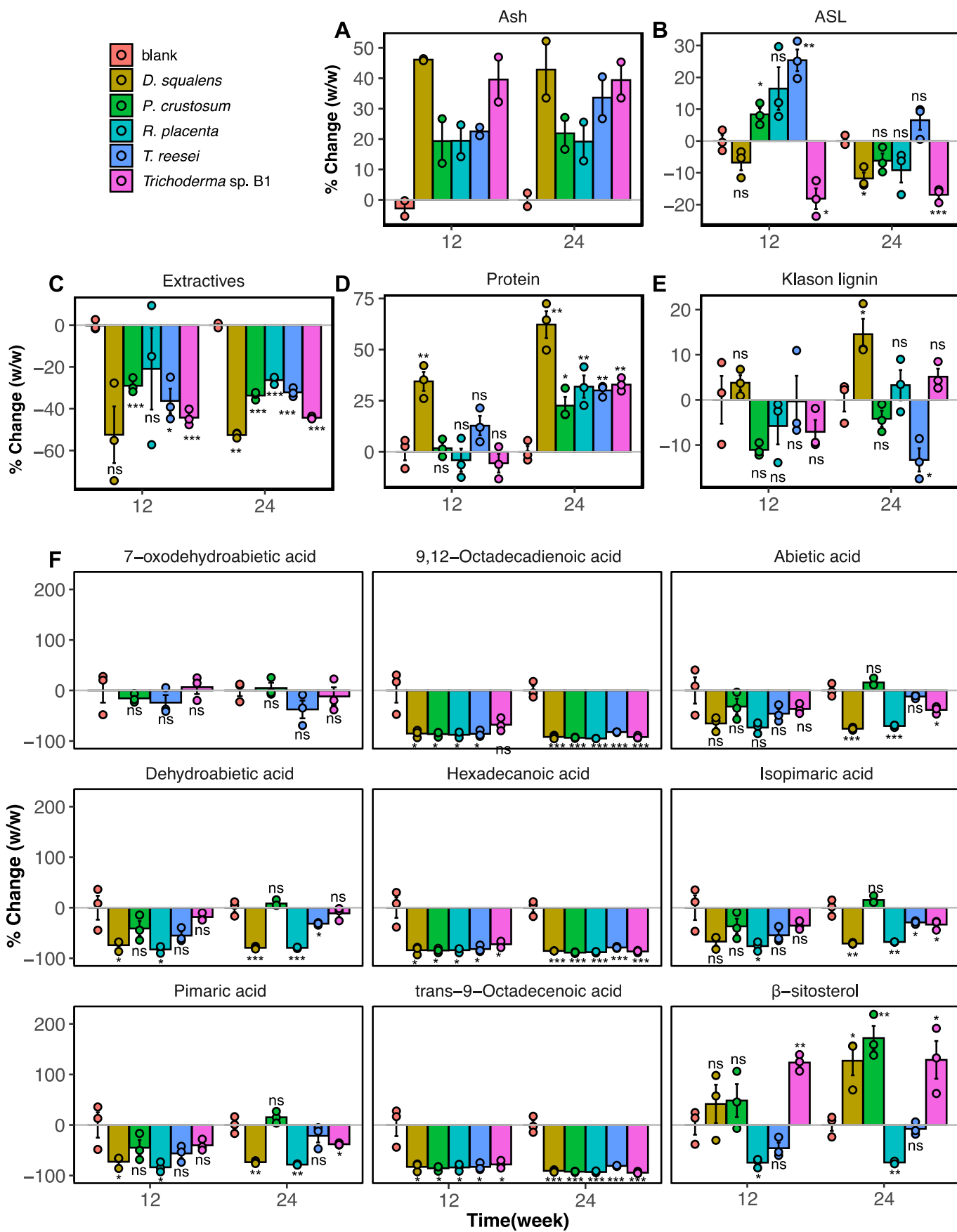
at 12 weeks (see supplementary material). Their consumption suggests them all deriving from the bark, and not the fungi themselves.

The resin acid dehydroabietic acid, the most abundant extractive component (9.9 mg/g bark), was efficiently converted by *D. squalens* and *R. placenta* resulting in an 80 % reduction after 12 weeks of growth. The same trend was found for abietic acid, isopimaric acid, and pimaric acid, while 7-oxodehydroabietic acid was not identified in these samples. Previous studies have shown that *R. placenta* degrades resin acids during growth on Scots pine wood (Belt et al., 2022). Interestingly, much smaller, and in some cases minimal effects on the levels of all resin acids were observed for the three Ascomycetes, *P. crustosum*, *Trichoderma* sp. B1, and *T. reesei*. This not only indicates an inability to degrade or modify resin acids, but also tolerance to their inhibitory effects. Only *D. squalens* and *R. placenta* degraded the pimarane-type resin acid isopimaric acid, in addition to abietic acid. Resin acid degradation has been somewhat investigated for bacteria, for which ability to degrade both pimarane and abietane resin acids is very rare (Martin et al., 1999). Pimarane-type resin acids are considered more toxic and resistant to degradation compared to abietane types, making the similar degradation of both types by the Basidiomycetes used in this study an interesting observation that could be studied further. However, whether the resin acids underwent complete degradation/metabolism or were transformed into less harmful metabolites that escaped detection cannot currently be determined. The mechanisms underlying the tolerance of the Ascomycetes towards resin acids are currently unclear, though a previous study comparing the transcriptome of *P. gigantea* grown on untreated and acetone-extracted milled loblolly pine wood showed upregulation of ABC efflux transporters for the former, which may contribute to such tolerance (Hori et al., 2014). The present study is the first report of marked differences in bark extractive responses across different fungal taxa.

As expected, the fungal cell membrane sterol ergosterol was identified only in fungus-treated bark samples. The most abundant bark-derived sterol,  $\beta$ -sitosterol, with an initial abundance of 2.6 mg/g bark, increased in cultures inoculated with *P. crustosum*, *D. squalens*, and *Trichoderma* sp. B1 (Fig. 2). This suggests that these fungi possess steryl esterases and can metabolize the released fatty acids but have limited ability to further degrade  $\beta$ -sitosterol itself. In contrast, *R. placenta* and, to a lesser extent, *T. reesei* were able to degrade  $\beta$ -sitosterol, indicating that they can metabolize both sterols and steryl esters. Steryl esters were unfortunately not possible to measure directly in this experimental setup.

### 3.4. Degradation of carbohydrates

To gain a comprehensive understanding of overall polysaccharide degradation, all samples were subjected to sulfuric acid hydrolysis followed by monosaccharide quantification using HPAEC-PAD (Fig. 3). The degradation of glucuronoarabinoxylan (GAX) and pectin was assessed by measuring the change in xylose (Xyl) and rhamnose (Rha) (initially 28.2 and 6.4 mg/g bark, respectively; see supplementary material). *D. squalens* and *P. crustosum* rapidly consumed Rha, in contrast to the two *Trichoderma* species. After 12 weeks, the white-rot *D. squalens* exhibited significant removal of Xyl (64 %) and Rha (66 %), indicating efficient degradation of both GAX and pectin. In contrast, the other Basidiomycete *R. placenta* displayed a clear preference for pectin degradation, with a similar removal of Rha (47 % and 62 % at week 12 and 24, respectively) as *D. squalens*, but less Xyl removal (15 % and 32 % after 12 and 24 weeks). *P. crustosum* exhibited an even greater preference for early-stage pectin degradation, removing 66 % of Rha at week 12, compared to 23 % for Xyl. In contrast to these three fungi, the two *Trichoderma* species showed limited degradation of pectin, Rha (~27 % removal after 24 weeks) and a preference for GAX degradation (~60 % Xyl removal after 24 weeks). *T. reesei* is a poor pectin degrader (Gao et al., 2022), but while *Trichoderma* sp. B1 grew on poly-methylgalacturonan on agar plates (unpublished results), spruce bark



(caption on next page)

**Fig. 2.** Effect of fungal treatment on bark components over 24 weeks of growth. A) Percent change in ash content in each chemically analyzed sample, showing a consistent increase across all samples subjected to fungal treatment. Panels B – E show the percent change in acid soluble lignin (B; ASL), acetone-soluble extractives (C), protein (D) Klason lignin (E) content after 12 and 24 weeks. Panel F shows the effect of fungal growth on the content of selected extractive compounds after 12 and 24 weeks of growth. This panel shows that fungal treatment led to decreases in the three fatty acids, hexadecanoic acid, 9,12-octadecadienoic acid and *trans*-9-octadecenoic acid, across all samples. The resin acids dehydroabietic acid, abietic acid, pimaric acid all decreased in the bark samples treated with the two Basidiomycetes *D. squalens* and *R. placenta*, while little to no change was observed for the three fungi from the Ascomycota phylum. 7-oxodehydroabietic acid was not identified in the bark samples treated with *D. squalens* or *R. placenta*.  $\beta$ -sitosterol increased in samples treated with *D. squalens*, *P. crustosum* and *Trichoderma* sp. B1 and was only degraded by *T. reesei*. Asterisks denote p-values compared to corresponding blank samples: ns = not significant, \* =  $p \leq 0.05$ , \*\*  $p \leq 0.01$ , \*\*\* =  $p \leq 0.001$ .

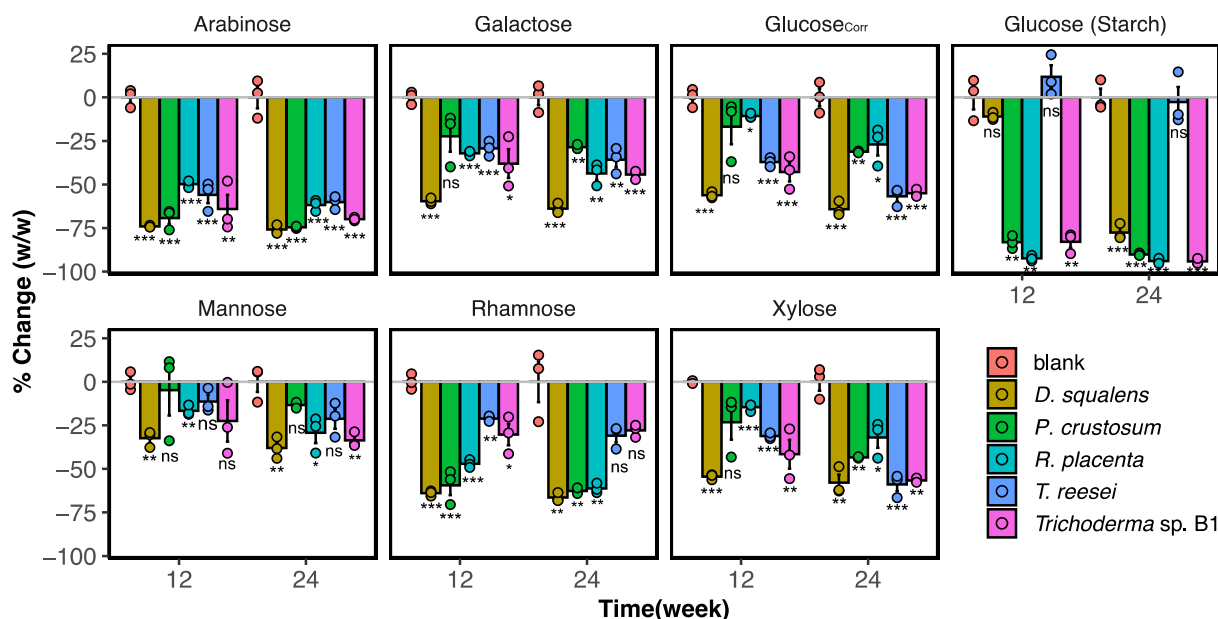


**Fig. 3.** Effect of fungal treatment on the arabinose, galactose, glucose<sub>corr</sub> = glucose corrected for measured glucose from starch, glucose (Starch) = measured starch content, mannose, rhamnose, and xylose composition of the bark after 12 and 24 weeks of fungal growth. The values were normalized against the total amount of ash, with the percent change relative to the blank sample for each timepoint (Eq. (1)). Data points from biological triplicate experiments are shown, with means and error bars (standard error). Data for the control (blank) samples are shown in the supplementary material. Asterisks denote p-values compared to corresponding blank samples: ns = not significant, \* =  $p \leq 0.05$ , \*\* =  $p \leq 0.01$ , \*\*\* =  $p \leq 0.001$ .

pectins may be too complex for efficient depolymerization in comparison. Xylan metabolism was relatively consistent among the fungi, except for *R. placenta* which showed weak xylan degradation.

After complete sulfuric acid hydrolysis of bark, arabinose (Ara) and galactose (Gal) (initial abundances 56.8 mg/g and 22.7 mg/g bark, respectively; see [supplementary material](#)), can derive from both pectin and the hemicelluloses GAX and GGM. Ara removal was observed for all five fungi ([Fig. 3](#)). In contrast, the degradation of Gal varied among the fungi. *D. squalens* reached a maximal degradation already at week 12 (64 % removal), a value the other fungi did not reach even after 24 weeks (~25–50 % removal). The removal of Man (initial amount 20.7 mg/g), derived from GGM, was seemingly limited for all fungi; *D. squalens* displayed the highest removal (37 % after 12 weeks). Importantly, consumption of bark-derived Man is likely underestimated as mannan is a major component of fungal biomass.

The spruce bark starch content was low (initially 5.41 mg/g), as in some previous studies ([Kemppainen et al., 2014](#); [Le Normand et al., 2012](#)) (see [supplementary material](#)). *R. placenta*, *Trichoderma* sp. B1, and *P. crustosum* degraded about 90 % of it by week 12 ([Fig. 3](#)). Intriguingly, *T. reesei* showed no starch degradation. *D. squalens* appeared to only have initiated starch degradation after twelve weeks, but showed major degradation at week 24. The results may be confounded by an accumulation of fungal glycogen, which is indistinguishable using this analytical approach. The remaining glucose (Glc<sub>corr</sub>), initially 243.7 mg/g (see [supplementary material](#)) when corrected for apparent starch content, comprises glucose (Glc) from cellulose, hemicellulose (GGM or possibly xyloglucan, XyG), and at later stages possibly from fungal

$\beta$ -glucans. By week 12, *D. squalens* achieved the highest Glc removal (64 %), with *Trichoderma* sp. B1 (56 %), and *T. reesei* (55 %) reaching similar levels. *R. placenta* and *P. crustosum* only achieved 25 % degradation at 24 weeks. Compared to a previous study on microbial consortia growing on spruce bark, where carbohydrate turnover was minimal despite the presence of Ascomycetes and Basidiomycetes ([Ristinmaa et al., 2023](#)), the isolated fungi used here showed significant degradation of polysaccharides. In a consortium, factors such as competition or direct bacterial inhibition of fungi may be highly important. The polysaccharide-degradation efficiency of *D. squalens* may reflect an overall synergistic effect, where broad simultaneous degradation gives better access to all polysaccharides compared to more selective degradation seen for other species, where parts of the spruce biomass may be ‘blocked’.

The *D. squalens* samples were subjected to methanolysis to gain additional insights. Again, changes in related monosaccharide levels between weeks 12 and 24 were minimal, indicating strong initial degradation (see [supplementary material](#)). Both 4-O-methyl-D-glucuronic acid and Xyl, associated with GAX (initial levels: 2.9 mg/g and 29 mg/g, respectively) decreased to similar extents (34 % and 44 % removal) after 12 weeks. Also clear removal of galacturonic acid (67 %), Rha (60 %), Ara (70 %), and Gal (55 %), associated with pectin, at week 12 (initial levels: 56, 8.9, 66.7, and 27 mg/g) was seen. Measurements of glucuronic acid (initially 2.3 mg/g) were highly variable, making estimation on removal (27 %) inconclusive. Subtraction of the total Glc concentration (sulfuric acid hydrolysis) from non-cellulosic Glc (methanolysis) indicates that cellulose degradation ceased after 12 weeks

when 61 % had been converted (timepoint zero = 159 mg/g).

### 3.5. Secretome composition during growth of *D. squalens* on spruce bark

It was evident that *D. squalens* displayed rapid growth on spruce bark and effectively degraded both extractives and polysaccharides. To further investigate which proteins the fungus produced during the degradation process, proteomics analysis was conducted. *D. squalens* was cultivated using five different carbon sources: spruce bark (Bark), acetone extracted spruce bark (extractive free; ACB), cellulose, galactomannan (GM), and glucose. A previously established plate method that facilitates the separation of secreted proteins (the secretome) and fungal biomass was employed (Bengtsson et al., 2016).

Proteins were annotated as extracellular if identified as such by at least two of three predictors (7.5 % of the whole proteome). A total of 1,139 proteins were identified in the experimental secretomes, with 193 (17 %) annotated as extracellular (see supplementary material). Extracellular protein fractions varied: 40 % for cellulose to approximately 17 % for ACB, Bark and GM, indicating different extents of lysis. For filamentous fungi, the plate method used can give varying degrees of enrichment of secreted proteins, depending on carbon source (Arntzen et al., 2020), and given the observed lysis in these samples, further analysis was limited to predicted extracellular proteins.

### 3.6. Extracellular carbohydrate-active enzymes produced by *D. squalens*

The secretomes were analyzed using dbCAN2 v11 (Zhang et al., 2018) to identify CAZymes. Out of the 193 identified predicted extracellular proteins, 105 were annotated as CAZymes, indicating a notable enrichment (for the predicted secretome, 22 % of proteins are CAZymes). Among these, the majority (n = 68; 65 %), were identified as glycoside hydrolases (GHs). Notably, there was no single CAZyme found in every secretome. Thirty detected CAZymes were found only in the hemicellulose-containing substrates (Bark, ACB, GM); these included 21 GHs. The compositional data, showing major degradation of pectin, cellulose, starch, GAX, and GGM was further supported by the detection of multiple members from glycoside hydrolase families GH28 (n = 5), GH7 (n = 3), GH31 (n = 3), GH5\_7 (n = 2), and GH10 (n = 4).

As expected, the secretomes for Bark, ACB, and cellulose contained multiple putative cellulose-degrading enzymes (Table 1), including  $\beta$ -glucosidases (GH3; n = 3), cellobiohydrolases (GH6/GH7; n = 4), endoglucanases (GH5/GH12; n = 10), AA3 cellobiose dehydrogenases (CDH, AA3\_1; n = 1), and lytic polysaccharide monoxygenase (LPMOs; AA9, n = 8). Remarkably, the secretomes for both bark substrates

**Table 1**

CAZymes identified in the *D. squalens* secretomes from growth on acetone-extracted bark (ACB), non-extracted bark (Bark), galactomannan (GM), cellulose (Cel) or glucose (Glc). The Table shows all CAZy families from which at least one member was detected and the number of identified members per family (see supplementary material). Abbreviations: AA, auxiliary activity; CE, carbohydrate esterase; GH, glycoside hydrolase. No Polysaccharide Lyases were detected.

Polysaccharide	CAZy family	ACB	Bark	GM	Cel	Glc
Cellulose	GH3*, 5, 6, 7, 12, 44	14	15	11	6	0
	AA9, AA3_1	5	9	3	2	0
Starch	GH13, 31*	1	2	3	0	0
Xylan	GH10	3	4	0	0	0
	CE2, 4, 15, 16	5	11	12	0	1
Xyloglucan	GH35, 74, 95, 12	5	4	4	2	1
Mannan	GH5_7, 27	3	5	5	1	0
Pectin	CE8	0	1	1	0	0
Lignin	GH28, 105, 43*, 53, 78	7	10	6	0	0
	AA1, 3.2, 5.1	5	6	5	0	0

\* These CAZyme families also contain members with other activities, meaning that the detected proteins could potentially be involved in depolymerization of other polysaccharides.

showed a higher number of AA9 LPMOs and cellobiohydrolases compared to the cellulose sample (Table 1; see supplementary material). Possibly, the higher complexity of bark leads to the production of more intricate enzymatic machineries. In this respect, it is noteworthy that AA9 LPMOs may act on various hemicelluloses and cellulose-hemicellulose assemblies (Frommshagen et al., 2015; Hüttner et al., 2019). Also, putative starch degrading enzymes were detected, including  $\alpha$ -amylase (GH13, n = 2) and  $\alpha$ -glucosidase (GH31, n = 3) in the Bark, ACB, and GM proteomes.

Degradation of the main spruce bark hemicelluloses GGM and GAX involves various enzymes, and in the secretomes  $\beta$ -xylosidase/ $\alpha$ -L-arabinofuranosidase (GH43; n = 2), xylanase (GH10; n = 4), endomannanase (GH5\_7; n = 2),  $\beta$ -mannosidase/glucosidase (GH2; n = 1), acetylxylan esterases (CE2/CE4; n = 2), and glucuronoyl esterases (CE15; n = 7) were detected (Table 1), except in the cellulose sample. The CEs detected play a role in deacetylating polysaccharides and breaking lignin-carbohydrate linkages between hemicellulose and lignin, possibly contributing to better accessibility for backbone degrading enzymes (Larsbrink & Lo Leggio, 2023). Surprisingly, enzymes putatively acting on xyloglucan (XyG), were identified in all proteomes. This included xyloglucanases (GH74/GH44; n = 2) and a fucosidase (GH95; n = 1). XyG was recently identified in spruce bark but not typically associated with bark tissue (Kempainen et al., 2014). The identification of enzymes capable of breaking down XyG during growth on bark serves as further evidence for the existence of XyG in spruce bark.

Predicted pectin-active CAZymes were identified, including polygalacturonases (GH28; n = 5), pectin methylesterase (CE8; n = 1), rhamnosidase (GH78; n = 1), endoarabinanase (GH43; n = 2), and rhamnogalacturonoyl hydrolase (GH105; n = 1). Interestingly, a larger number of proteins from these pectin-related families were identified in the two bark samples (Table 1), which corresponds well with pectin being a part of the bark matrix.

While Basidiomycetes are recognized for their ability to metabolize lignin, the analyses suggested lignin degradation being limited and as discussed above, only 10 % of ASL appeared to be removed over the six month-long experiment with *D. squalens*. Nevertheless, in the proteomes, predicted lignin-degrading enzymes were identified in both bark proteomes, with oxidoreductases (AA3\_2; n = 4), copper radical oxidases (AA5\_1; n = 2), and laccases (AA1; n = 2). Surprisingly, five of these seven proteins were found in the GM as well as the two bark samples, possibly suggesting co-regulation of GM- and lignin degradation. Putative chitinolytic enzymes were also found, with  $\beta$ -N-acetylhexosaminidase (GH20; n = 2), chitinase (GH18; n = 3),  $\alpha$ -N-acetylglucosaminidase (GH89; n = 1), and chitin deacetylase esterase (CE4; n = 1), identified in the Bark, ACB, and GM proteomes, possibly reflecting fungal cell wall modification during growth.

### 3.7. Extracellular proteins detected during growth on spruce bark

Of all 193 proteins predicted to be secreted, 42 were exclusively identified in both bark samples (Fig. 4; see supplementary material) and 31 of these were annotated as CAZymes (Fig. 4). Fewer proteins were detected in the ACB proteome compared to non-extracted bark, which could reflect that ACB is less complex. Many GHs (11 out of 20 total detected) were found in both extractive-free and the non-treated bark samples, and 8 exclusively in the latter. Only one GH, a putative GH115  $\alpha$ -glucuronidase (UniProt accession number; A0A4Q9PZ29) was exclusively found in ACB sample.

As expected from observed degradation of GAX and pectin, some putative xylan and pectin degrading enzymes were identified only in the bark proteomes and several only in non-extracted bark, including:  $\alpha$ -(1 $\rightarrow$ 2)-L-fucosidase (GH95, A0A4V2K8L7),  $\alpha$ -L-rhamnosidase (GH78, A0A4Q9PG03), and polygalacturonase (GH28, A0A4Q9NRD1). Two GH10 xylanases (A0A4Q9PNM1, A0A4V2K1M9) were found in both bark samples. Several GHs putatively related to fungal cell-wall

**A**

UniProt accession	CAZyme	Protein name	ACB	Bark	Class
<b>A0A4Q9Q8S7</b>		DUF1793-domain-containing protein	Yes	Yes	N/A
A0A4Q9PS69		Glycoside hydrolase family 43 protein	Yes	Yes	N/A
<b>A0A4Q9PLQ5</b>		Six-hairpin glycosidase-like protein	Yes	Yes	N/A
A0A4Q9QAL2	AA9	Endo-β-1,4-glucanase D (Endoglucanase D)	Yes	Yes	GH
A0A4Q9P7M4	AA1	Laccase	Yes	Yes	AA
A0A4V2K8L7	GH95	Six-hairpin glycosidase-like protein	Yes	Yes	N/A
A0A4Q9QAY2	GH79	Glyco_hydro_79C domain-containing protein	Yes	Yes	N/A
A0A4Q9PG03	GH78	Six-hairpin glycosidase	Yes	Yes	N/A
A0A4V2K7E2	GH44	Glycoside hydrolase family 44-domain-containing protein	Yes	Yes	N/A
A0A4Q9PTR3	GH43	Arabinan endo-1,5-α-L-arabinosidase	Yes	Yes	N/A
A0A4Q9PQB7	GH31	α-glucosidase	Yes	Yes	N/A
A0A4Q9NRD1	GH28	Pectin lyase fold/virulence factor	Yes	Yes	N/A
A0A4Q9PNM1	GH10	β-xylanase	Yes	Yes	N/A
A0A4V2K1M9	GH10	β-xylanase	Yes	Yes	N/A
A0A0U3CB12	GH6	Glucanase	Yes	Yes	N/A
A0A4Q9QB99	CBM1+GH3	β-glucosidase	Yes	Yes	N/A
A0A4Q9PGE8	CE2	SGNH hydrolase	Yes	Yes	CE
A0A4Q9PSB3		Actin-like ATPase domain-containing protein	Yes	Yes	N/A
<b>A0A4Q9P6Q6</b>		DUF1793-domain-containing protein	Yes	Yes	N/A
A0A4Q9PAG2		Oligoxyloglucan reducing end-specific cellobiohydrolase	Yes	Yes	N/A
A0A4Q9MED4		Dolichyl-diphosphooligosaccharide	Yes	Yes	N/A
<b>A0A4V2K8F9</b>		Cytochrome P450	Yes	Yes	N/A
A0A4V2K7T4		Hydrophobic surface binding protein A	Yes	Yes	N/A
A0A4V2K7A4		Peptide hydrolase	Yes	Yes	N/A
A0A4Q9Q8Z1	AA9	Endo-β-1,4-glucanase D (Endoglucanase D)	Yes	Yes	GH
A0A4Q9PQC0	AA9+CBM1	Endo-β-1,4-glucanase D (Endoglucanase D)	Yes	Yes	GH
A0A4Q9MYB6	AA9	Endo-β-1,4-glucanase D (Endoglucanase D)	Yes	Yes	GH
A0A4Q9MRJ0	AA7	FAD dependent oxidoreductase	Yes	Yes	N/A
A0A4Q9NTH3	AA5_1	Glyoxal oxidase N-terminus-domain-containing protein	Yes	Yes	N/A
A0A4Q9P514	AA3_2	Endo-β-1,4-glucanase D (Endoglucanase D)	Yes	Yes	GH
A0A4Q9P6J3	GH125	Six-hairpin glycosidase-like protein	Yes	Yes	N/A
A0A4Q9PQL0	CBM1+GH131	CBM1 domain-containing protein	Yes	Yes	N/A
A0A4Q9PXC4	GH105	Six-hairpin glycosidase-like protein	Yes	Yes	N/A
A0A4Q9PUY3	CBM5+GH18	Glycosyl hydrolases family 18-domain-containing protein	Yes	Yes	N/A
A0A4Q9NZH8	CBM20+GH13_32	α-amylase	Yes	Yes	N/A
A0A4Q9P532	GH10	β-xylanase	Yes	Yes	N/A
A0A4Q9Q1N2	GH5_5	Endoglucanase	Yes	Yes	N/A
A0A4Q9Q5A1	GH5_9	Exo-β-1,3-glucanase	Yes	Yes	N/A
A0A4V2K6I0	CE16	Carbohydrate esterase family 16 protein	Yes	Yes	CE
A0A4Q9P1R1	AA3_2	Alcohol oxidase	Yes	Yes	AA
<b>A0A4Q9PML4</b>		Uncharacterized protein	Yes	Yes	N/A
A0A4Q9PZ29	GH115	GH115_C domain-containing protein	Yes	Yes	N/A

**B**

**Fig. 4.** Proteins predicted to be secreted and that were identified in the secretome of *D. squalens* during growth on bark or acetone-extracted bark (ACB). A) List of the secreted proteins only detected in one or both of the bark proteomes. Proteins that were not detected on a specific carbon source are colored grey in the grid and proteins detected are colored blue. Protein accession numbers (Uniprot), CAZy annotations (by dbCAN2) and protein names (from Uniprot) are shown (note that there are some minor inconsistencies between the Uniprot- and dbCAN2-based annotations). When applicable, the CAZy class is indicated in the right column by color: AA (auxiliary activity) in pink, CE (carbohydrate esterase) in green, GH (glycoside hydrolase) in blue, N/A in grey. The higher abundance and diversity of secreted proteins during growth on intact bark compared to extractive-free bark is apparent, both regarding putative hydrolases and oxidoreductases. B) Domain architecture of five hypothetical proteins only found in one or both of the bark proteomes (indicated in bold in A). Signal peptides are shown in yellow. DUF = domain of unknown function. (For interpretation of the references to color in this figure legend, the reader is referred to the web version of this article.)

modification were also identified, including an *exo*-α-(1→6)-mannosidase (GH125, A0A4Q9P6J3) and a chitinase (GH18, A0A4Q9PUY3). It is conceivable that the bark extractives induced lysis, stimulating the fungus to reinforce and/or adapt its cell wall, though the

presence of these enzymes could also reflect general cell wall modification during growth.

Of the nine secreted proteins classified as auxiliary activity (AA) detected in the bark samples, six were found only in the non-extracted

bark proteome, including 3 out of the 4 AA9 LPMOs (A0A4Q9PQC0, A0A4Q9Q8Z1, A0A4Q9QAL2). While LPMOs are commonly linked to cellulose degradation, recent research has unveiled their activity on cellulose-associated xylan (Frommhagen et al., 2015; Hüttner et al., 2019). Some AA9 LPMOs can also oxidize phenolic compounds or contribute indirectly by supplying other enzymes with H<sub>2</sub>O<sub>2</sub> through their oxidase activity (Kracher et al., 2016; Li et al., 2021). The proteome from non-extracted bark contained additional H<sub>2</sub>O<sub>2</sub>-producing enzymes: AA3\_2 glucose oxidase (A0A4Q9P514), AA5\_1 glyoxal oxidase (A0A4Q9NTH3), and AA7 oligosaccharide oxidase (A0A4Q9MRJ0). Produced H<sub>2</sub>O<sub>2</sub> could drive LMPO reactions (Bissaro et al., 2017), or enable unspecific Fenton reactions which can drive degradation of pine extractives (Belt et al., 2022; Belt et al., 2017). Both LPMO and Fenton reactions also require reducing power that likely can be delivered by certain extractives, as has been demonstrated for gallic acid (Golten et al., 2023). One laccase (AA1, A0A4Q9P7M4) was present in both bark samples, and could possibly be involved in conversion of lignin or, maybe more likely, extractives.

Several proteins of unknown function were identified only in the bark samples (Fig. 4), which is a strong indication that they have bark-related functions. Eleven of the 42 bark-specific proteins have no CAZY annotation, and seven of these were only found in the non-extracted bark sample. Putative annotations of these using Uniprot and dbCAN indicate possible novel CAZymes, with a six-hairpin glycosidase-like protein (A0A4Q9PLQ5), a putative GH43 protein (A0A4Q9PS69), and a reducing-end specific xyloglucan oligosaccharide hydrolase (A0A4Q9PAG2). Additionally, an uncharacterized protein (A0A4Q9PML4), two proteins with domains of unknown function (DUFs) (A0A4Q9Q8S7, A0A4Q9P6Q6), and a cytochrome P450 (A0A4V2K8F9) were identified. A0A4Q9PLQ5 showed high sequence identity (75.84 %) to a GH65 protein (A0A5C3PMI1) from *Polyporus arcularius*, which however has not been biochemically characterized, making functional prediction speculative (of note, GH65 contains a wide variety of catalytic activities). A0A4Q9PML4 has no clear functional prediction, but the closest hits to an AlphaFold model in Dali are a nuclease and a member from the Plant Invertase/Pectin Methyltransferase Inhibitor superfamily (Holm, 2020). The top hits for the AlphaFold model of A0A4Q9Q8S7 in Dali were a glucosylceramidase and a  $\beta$ -xylosidase (Holm, 2020). The two DUF proteins A0A4Q9Q8S7 and A0A4Q9P6Q6, categorized as carbohydrate metabolic process proteins (Interpro), actually comprise three DUFs (DUF5127, 4965, and 1793; Pfam: PF17168, PF16335, PF08760), with the two C-terminal domains similar to six-hairpin glycosidases (residues 391–582). Possibly, both proteins function as GHs, as they are similar in architecture to WP\_074995790 from *Streptomyces misionensis*, which has weak  $\beta$ -galactosidase activity (Schmerling et al., 2022).

Although assignment of functionality requires biochemical characterization, several of the proteins with unknown function detected in the bark secretomes may be involved in carbohydrate turnover. The notable exception is the cytochrome P450 protein, A0A4V2K8F9, only detected with non-extracted bark, which possibly has a role in the modification of spruce extractives. Previously, *R. placenta* was shown to upregulate cytochrome P450s during growth on pinewood, suggesting that oxidative processes are important during growth on softwood biomass (Vanden Wymelenberg et al., 2011).

#### 4. Conclusions

Understanding of microbial bark degradation is fundamental to develop biological utilization processes. Fungi from various taxonomic groups were shown able to grow on spruce bark, using different growth and degradation strategies. Among the five fungi, *D. squalens*, *T. reesei*, and *Trichoderma* sp. B1 were the most efficient in overall bark degradation, especially regarding extractives, pectin, GAX, and starch. Proteomics analysis of *D. squalens* implicated multiple putative CAZymes and proteins of unknown function that could be involved in

polysaccharide and extractive degradation. This work provides a foundation for further valorization of this abundant renewable resource.

#### Funding information

Funding was provided by an energy-oriented basic research grant from the Swedish Energy Agency and the Swedish Research Council (project number 46559–1) awarded to J.L. MØA was supported by the Novo Nordisk Foundation through grant NNF20OC0061313.

#### CRediT authorship contribution statement

**Amanda S. Ristinmaa:** Writing – review & editing, Writing – original draft, Visualization, Validation, Resources, Project administration, Methodology, Funding acquisition, Formal analysis, Conceptualization. **Ekaterina Korotkova:** Methodology, Formal analysis. **Magnus Ø. Arntzen:** Vincent G. H. Eijsink: Writing – review & editing, Methodology. **Chunlin Xu:** Writing – review & editing, Methodology. **Anna Sundberg:** Writing – review & editing, Methodology. **Merima Hasani:** Writing – review & editing, Validation, Supervision, Resources, Methodology, Funding acquisition. **Johan Larsbrink:** Writing – review & editing, Validation, Supervision, Resources, Project administration, Methodology, Funding acquisition, Formal analysis, Conceptualization.

#### Declaration of competing interest

The authors declare that they have no known competing financial interests or personal relationships that could have appeared to influence the work reported in this paper.

#### Data availability

Data will be made available on request.

#### Acknowledgements

This work was performed in part at the Chalmers Material Analysis Laboratory, CMAL. We thank Marcel Taillefer for helpful discussions. Proteomics analyses were performed by The MS and Proteomics Core Facility, Norwegian University of Life Sciences (NMBU). This facility is a member of the National Network of Advanced Proteomics Infrastructure (NAPI), which is funded by the Research Council of Norway INFRASTRUKTUR-program (project number: 295910).

#### Appendix A. Supplementary data

Supplementary data to this article can be found online at <https://doi.org/10.1016/j.biortech.2024.130768>.

#### References

- Arntzen, M.Ø., Bengtsson, O., Várnai, A., Delogu, F., Mathiesen, G., Eijsink, V.G.H., 2020. Quantitative comparison of the biomass-degrading enzyme repertoires of five filamentous fungi. *Sci. Rep.* 10 (1), 20267.
- Belt, T., Harju, A., Kilpeläinen, P., Venäläinen, M. 2022. Fungal degradation of extractives plays an important role in the brown rot decay of Scots pine heartwood. *Frontiers in Plant Science*, 1574.
- Belt, T., Hänninen, T., Rautkari, L., 2017. Antioxidant activity of Scots pine heartwood and knot extractives and implications for resistance to brown rot. *Holzforchung* 71 (6), 527–534.
- Bengtsson, O., Arntzen, M.Ø., Mathiesen, G., Skaugen, M., Eijsink, V.G.H., 2016. A novel proteomics sample preparation method for secretome analysis of *Hypocrea jecorina* growing on insoluble substrates. *J. Proteomics* 131, 104–112.
- Bissaro, B., Röhr, Å.K., Müller, G., Chylenski, P., Skaugen, M., Forsberg, Z., Horn, S.J., Vaaje-Kolstad, G., Eijsink, V.G., 2017. Oxidative cleavage of polysaccharides by monooxygenase enzymes depends on H<sub>2</sub>O<sub>2</sub>. *Nat. Chem. Biol.* 13 (10), 1123–1128.
- Daly, P., López, S.C., Peng, M., Lancefield, C.S., Purvine, S.O., Kim, Y.M., Zink, E.M., Dohnalkova, A., Singan, V.R., Lipzen, A., 2018. *Dichomitus squalens* partially tailors its molecular responses to the composition of solid wood. *Environ. Microbiol.* 20 (11), 4141–4156.

- Ek, M., Gellerstedt, G., Henriksson, G. 2009. in: *Wood chemistry and biotechnology*. (Eds.) M. Ek, G. Gellerstedt, G. Henriksson. Walter de Gruyter, pp. 147-173.
- Fengel, D., Wegener, G., 1984. in: *Wood: chemistry*. In: Fengel, D., Wegener, G. (Eds.), *Ultrastructure, Reactions*. Gruyter, Walter de, pp. 227-238.
- Frommshagen, M., Sforza, S., Westphal, A.H., Visser, J., Hinz, S.W., Koetsier, M.J., van Berkel, W.J., Gruppen, H., Kabel, M.A., 2015. Discovery of the combined oxidative cleavage of plant xylan and cellulose by a new fungal polysaccharide monoxygenase. *Biotechnol. Biofuels* 8 (1), 1-12.
- Gao, L., Liu, G., Zhao, Q., Xiao, Z., Sun, W., Hao, X., Liu, X., Zhang, Z., Zhang, P., 2022. Customized optimization of lignocellulolytic enzyme cocktails for efficient conversion of pectin-rich biomass residues. *Carbohydr Polym* 297, 120025.
- Golten, O., Ayuso-Fernández, L., Hall, K.R., Stepnov, A.A., Sørli, M., Røhr, Å.K., Eijsink, V.G., 2023. Reductants fuel lytic polysaccharide monoxygenase activity in a pH-dependent manner. *FEBS Lett.* 1363-1374.
- Holm, L., 2020. DALI and the persistence of protein shape. *Protein Sci.* 29 (1), 128-140.
- Hori, C., Ishida, T., Igarashi, K., Samejima, M., Suzuki, H., Master, E., Ferreira, P., Ruiz-Dueñas, F.J., Held, B., Canessa, P., 2014. Analysis of the *Phlebiopsis gigantea* genome, transcriptome and secretome provides insight into its pioneer colonization strategies of wood. *PLoS Genet.* 10 (12), e1004759.
- Horton, P., Park, K.-J., Obayashi, T., Fujita, N., Harada, H., Adams-Collier, C., Nakai, K., 2007. WoLF PSORT: protein localization predictor. *Nucleic Acids Res.* 35, W585-W587.
- Hüttner, S., Várnai, A., Petrović, D.M., Bach, C.X., Kim Anh, D.T., Thanh, V.N., Eijsink, V. G.H., Larsbrink, J., Olsson, L., 2019. Specific xylan activity revealed for aa9 lytic polysaccharide monoxygenases of the thermophilic fungus *Malbranchea cinnamomea* by functional characterization. *Appl Environ Microbiol* 85, e01408-e01419.
- Jones, D.B. 1931. *Factors for converting percentages of nitrogen in foods and feeds into percentages of proteins*. US Department of Agriculture Circular Series, 183, 1-21.
- Käll, L., Krogh, A., Sonnhammer, E.L., 2004. A combined transmembrane topology and signal peptide prediction method. *J. Mol. Biol.* 338 (5), 1027-1036.
- Kemppainen, K., Siika-aho, M., Pattathil, S., Giovando, S., Kruus, K., 2014. Spruce bark as an industrial source of condensed tannins and non-cellulosic sugars. *Ind. Crop. Prod.* 52, 158-168.
- Kracher, D., Scheiblbrandner, S., Felice, A.K., Breslmayr, E., Preims, M., Ludwicka, K., Haltrich, D., Eijsink, V.G., Ludwig, R., 2016. Extracellular electron transfer systems fuel cellulose oxidative degradation. *Science* 352 (6289), 1098-1101.
- Krogell, J., Holmbom, B., Pranovich, A., Hemming, J., Willför, S., 2012. Extraction and chemical characterization of Norway spruce inner and outer bark. *Nord. Pulp Pap. Res. J.* 27 (1), 6-17.
- Krogell, J., Korotkova, E., Eränen, K., Pranovich, A., Salmi, T., Murzin, D., Willför, S., 2013. Intensification of hemicellulose hot-water extraction from spruce wood in a batch extractor - Effects of wood particle size. *Bioresour. Technol.* 143, 212-220.
- Kwan, I., Huang, T., Ek, M., Seppänen, R., Skagerlind, P., 2022. Bark from Nordic tree species - a sustainable source for amphiphilic polymers and surfactants. *Nord. Pulp Pap. Res. J.* 37 (4), 566-575.
- Larsbrink, J., Lo Leggio, L., 2023. Glucuronoyl esterases - enzymes to decouple lignin and carbohydrates and enable better utilization of renewable plant biomass. *Essays Biochem* 67 (3), 493-503.
- Le Normand, M., Edlund, U., Holmbom, B., Ek, M., 2012. Hot-water extraction and characterization of spruce bark non-cellulosic polysaccharides. *Nord. Pulp Pap. Res. J.* 27 (1), 18-23.
- Le Normand, M., Rietzler, B., Vilaplana, F., Ek, M., 2021. Macromolecular model of the pectic polysaccharides isolated from the bark of Norway spruce (*Picea abies*). *Polymers* 13 (7), 1106.
- Li, F., Zhao, H., Shao, R., Zhang, X., Yu, H., 2021. Enhanced Fenton reaction for xenobiotic compounds and lignin degradation fueled by quinone redox cycling by lytic polysaccharide monoxygenases. *J. Agric. Food Chem.* 69 (25), 7104-7114.
- Lorentzen, S.B., Arntzen, M.Ø., Hahn, T., Tuveng, T.R., Sørli, M., Zibek, S., Vaaje-Kolstad, G., Eijsink, V.G.H., 2021. Genomic and proteomic study of *Andreprevotia ripae* isolated from an anthill reveals an extensive repertoire of chitinolytic enzymes. *J. Proteome Res.* 20 (8), 4041-4052.
- Martin, V.J., Yu, Z., Mohn, W.W., 1999. Recent advances in understanding resin acid biodegradation: microbial diversity and metabolism. *Arch. Microbiol.* 172 (3), 131-138.
- Ristinmaa, A.S., Tafur Rangel, A., Idström, A., Valenzuela, S., Kerkhoven, E.J., Pope, P.B., Hasani, M., Larsbrink, J., 2023. Resin acids play key roles in shaping microbial communities during degradation of spruce bark. *Nat Commun* 14 (1), 8171.
- Schmerling, C., Sewald, L., Heilmann, G., Witfeld, F., Begerow, D., Jensen, K., Bräsen, C., Kaschani, F., Overkleef, H.S., Siebers, B., Kaiser, M., 2022. Identification of fungal lignocellulose-degrading biocatalysts secreted by *Phanerochaete chrysosporium* via activity-based protein profiling. *Communications Biology* 5 (1), 1254.
- Teufel, F., Almagro Armenteros, J.J., Johansen, A.R., Gíslason, M.H., Pihl, S.I., Tsirigos, K.D., Winther, O., Brunak, S., von Heijne, G., Nielsen, H., 2022. SignalP 6.0 predicts all five types of signal peptides using protein language models. *Nat. Biotechnol.* 40 (7), 1023-1025.
- Valentín, L., Kluczek-Turpeinen, B., Willför, S., Hemming, J., Hatakka, A., Steffen, K., Tuomela, M., 2010. Scots pine (*Pinus sylvestris*) bark composition and degradation by fungi: Potential substrate for bioremediation. *Bioresour. Technol.* 101 (7), 2203-2209.
- Vanden Wymelenberg, A., Gaskell, J., Mozuch, M., BonDurant, S.S., Sabat, G., Ralph, J., Skyba, O., Mansfield, S.D., Blanchette, R.A., Grigoriev, I.V., Kersten, P.J., Cullen, D., 2011. Significant alteration of gene expression in wood decay fungi *Postia placenta* and *Phanerochaete chrysosporium* by plant species. *Appl Environ Microbiol* 77 (13), 4499-4507.
- Yadav, K., Yadav, S., Anand, G., Yadav, P.K., Yadav, D. 2023. Hydrolysis of complex pectin structures: Biocatalysis and bioproducts. in: *Polysaccharide Degrading Biocatalysts*, Elsevier, pp. 205-225.
- Zhang, H., Yohe, T., Huang, L., Entwistle, S., Wu, P., Yang, Z., Busk, P.K., Xu, Y., Yin, Y., 2018. dbCAN2: a meta server for automated carbohydrate-active enzyme annotation. *Nucleic Acids Res.* 46 (W1), W95-W101.